

In-situ Generated of $Ti_3C_2T_x$ ($T_x=F, O$ and OH) MXene Decorated CuO Nanocomposite with Extraordinary Catalytic Activity for TKX-50 Thermal Decomposition

Dongqi Liu^a, Qiangqiang Lu^a, Chunlei Xuan^a, Lei Xiao^a, Fengqi Zhao^b, Xiaojun Feng^b, Kun Zhang^b, Jun Di^{*a}, Wei Jiang^{*a}, Gazi Hao^{*a}

(a: National Special Superfine Powder Engineering Research Center of China, School of Chemistry and Chemical Engineering, Nanjing University of Science and Technology, Nanjing 210094, China.)

(b: Xi' an Modern Chemistry Research Institute, Xi' an 710065, China.)

*corresponding author.

Email: dijun@njust.edu.cn (J. Di). superfine_jw@126.com (W. Jiang). hgznjust1989@163.com (G. Hao).

Supporting Information

Measurement conditions

Powder X-ray diffraction (XRD) was performed using a Rigaku smartlab 9 with Rigaku's original cross beam optics system (rated voltage of 40 kV, rated current of 150 mA). Field emission scanning electron microscopy (FESEM) (ZEISS GeminiSEM 500, Germany) was used to observe GO, Ti_3AlC_2 , $Ti_3C_2T_x$, CuO etc.. X-ray photoelectron spectroscopy (XPS) measurements were carried out on an ESCALAB 250Xi spectrometer (Thermo Scientific, USA) equipped with a pass energy of 30 eV with a power of 100 W (10 kV and 10 mA) and a monochromatized Al $K\alpha$ X-ray ($h\nu = 1486.65$ eV) source. All samples were analyzed under a pressure of less than 1.0×10^{-9} Pa. Spectra were acquired using Avantage software (Version 5.979) with a step of 0.05 eV. Raman spectra were obtained using a Raman spectrometer (LabRAM HR Evolution, HORIBA JobinYvon, France) at room temperature using the 532 nm line as the excitation source. The thermal analysis experiment was conducted using METTLER TOLEDO TGA/DSC3⁺; the N_2 flow rate was 50 ml/min; the selected heating rate were 5, 10, 15, and 20°C/min and the program heated from 50°C to 350°C.

Experimental Section

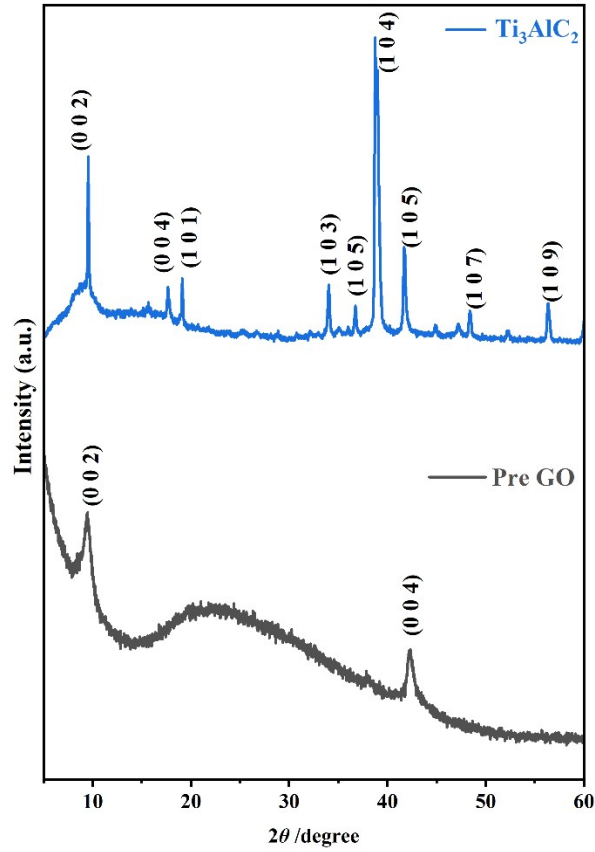


Fig. S1. XRD patterns of Pre GO (Graphite oxide) and Ti_3AlC_2

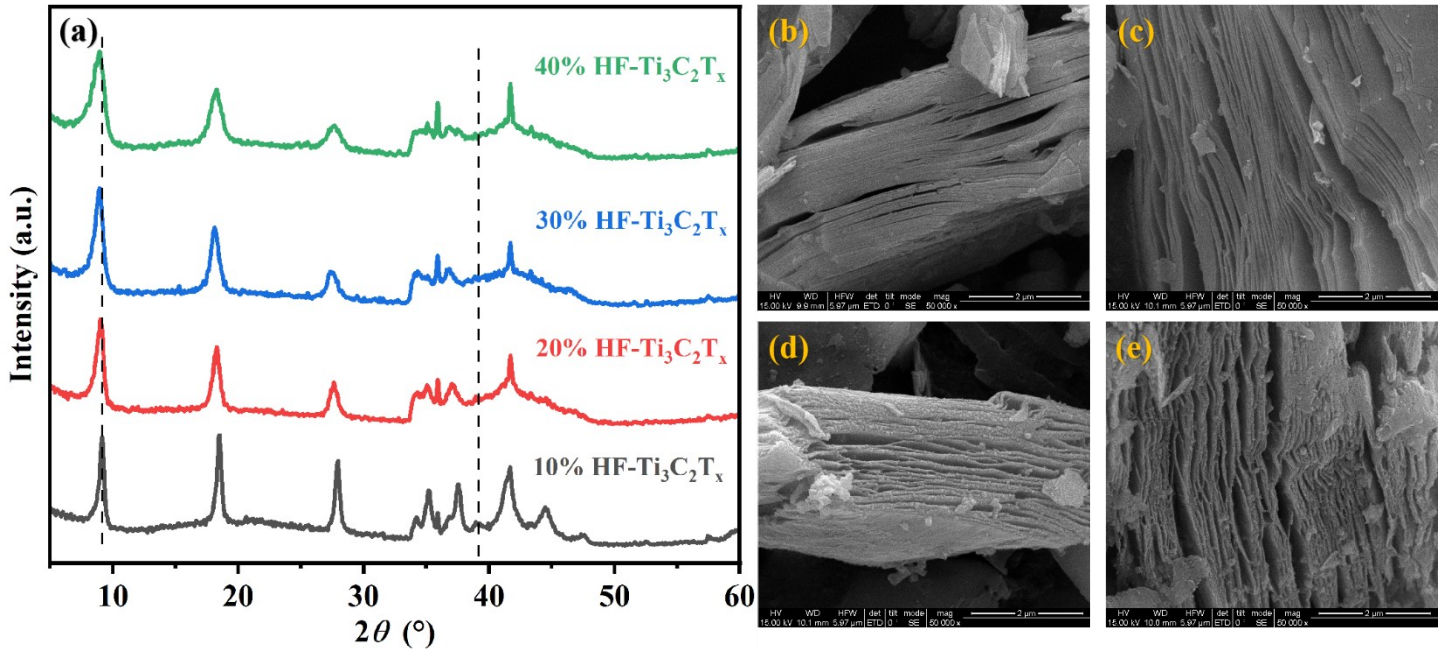
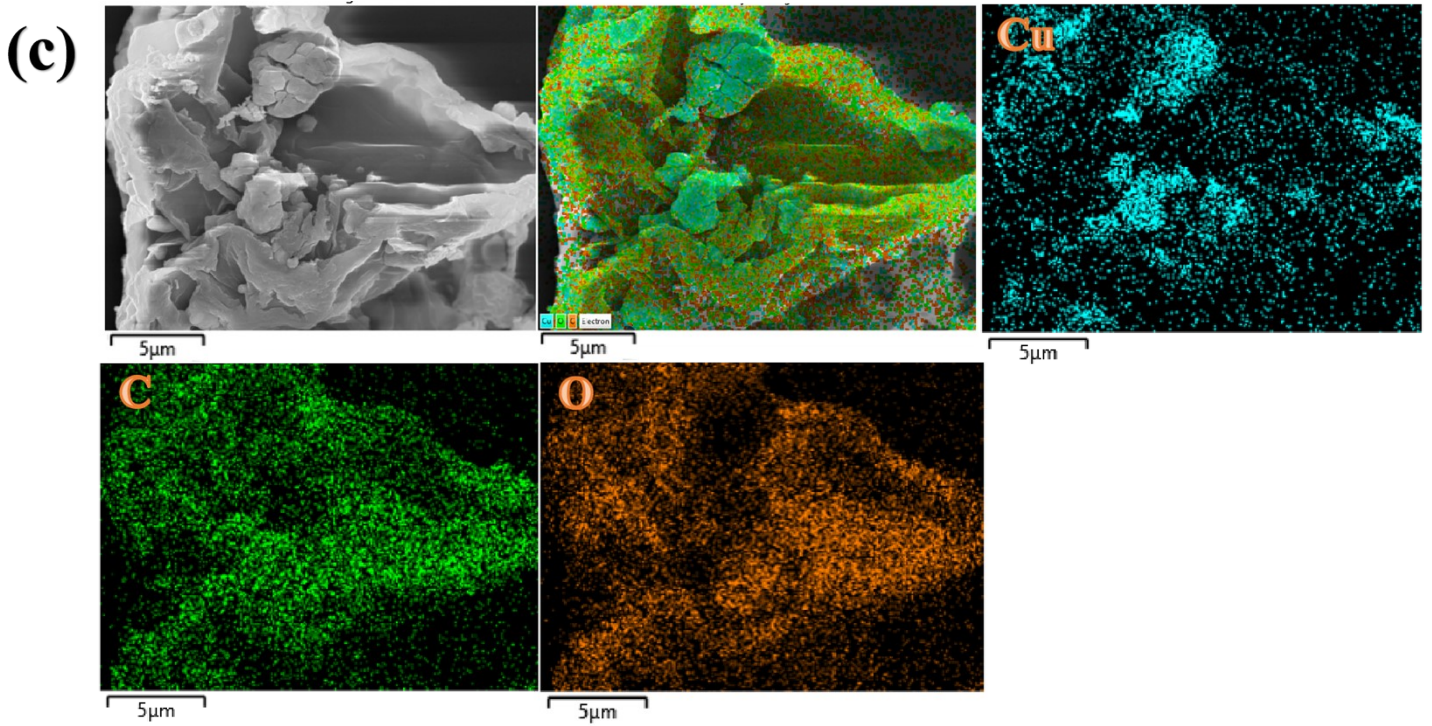
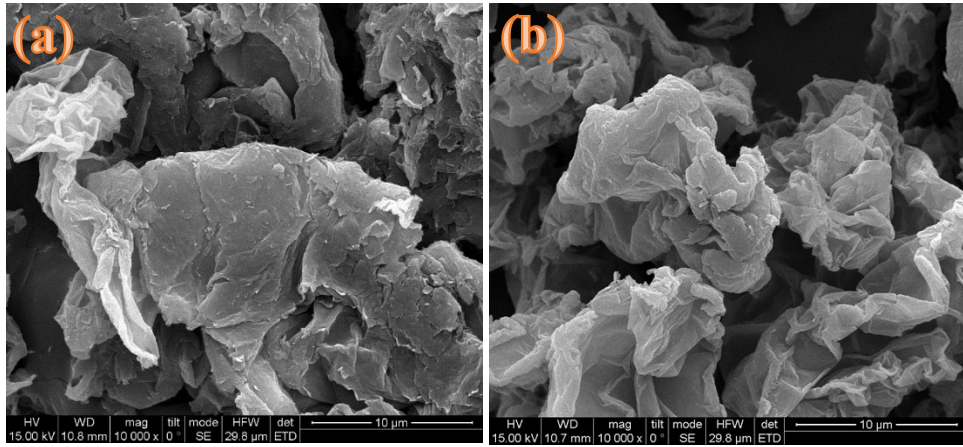


Fig. S2. (a) XRD patterns of 10%HF- $\text{Ti}_3\text{C}_2\text{T}_x$, 20%HF- $\text{Ti}_3\text{C}_2\text{T}_x$, 30%HF- $\text{Ti}_3\text{C}_2\text{T}_x$, 40%HF- $\text{Ti}_3\text{C}_2\text{T}_x$. SEM images of (b) 10%HF- $\text{Ti}_3\text{C}_2\text{T}_x$, (c) 20%HF- $\text{Ti}_3\text{C}_2\text{T}_x$, (d) 30%HF- $\text{Ti}_3\text{C}_2\text{T}_x$, (e) 40%HF- $\text{Ti}_3\text{C}_2\text{T}_x$.



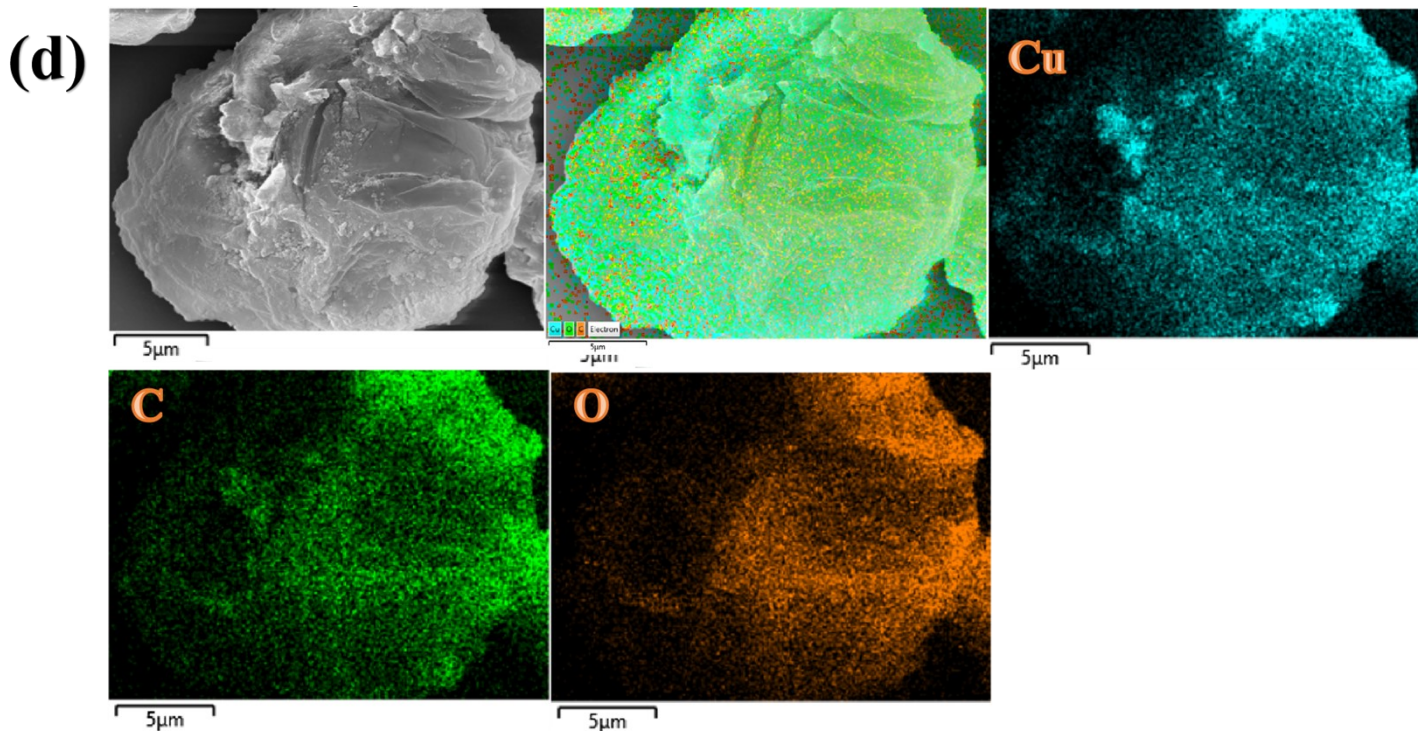
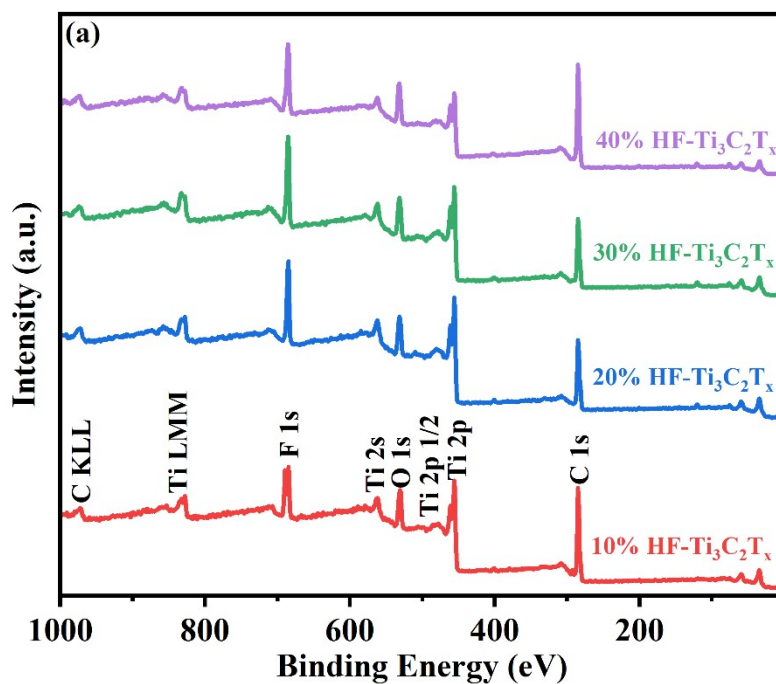


Fig. S3. SEM images of (a) Pre GO, (b) GO, (c) SEM images of GO/CuO composite and corresponding Cu, O, C elemental mapping. (d) SEM images of I-GO/CuO composite and corresponding Cu, O, C elemental mapping

As can be seen from **Fig. S4**, with the increase of HF etching concentration, the element distribution and valence states on the surface of $\text{Ti}_3\text{C}_2\text{T}_x$ MXene change little, thus exerting a little influence on it¹.



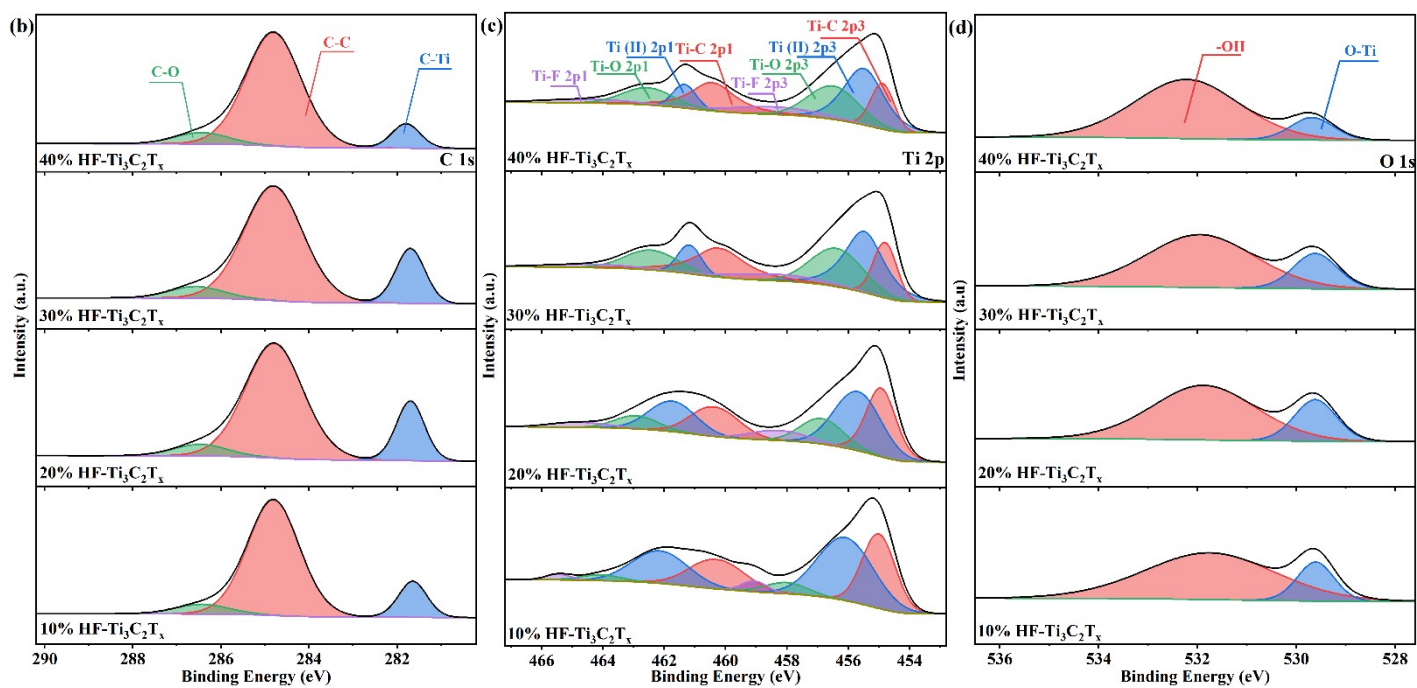


Fig. S4. XPS survey spectra of (a) 10%HF-Ti₃C₂T_x, 20%HF-Ti₃C₂T_x, 30%HF-Ti₃C₂T_x, 40%HF-Ti₃C₂T_x. High-resolution XPS spectra of (b) C 1s, (c) Ti 2p and (d) O 1s of 10%HF-Ti₃C₂T_x, 20%HF-Ti₃C₂T_x, 30%HF-Ti₃C₂T_x, 40%HF-Ti₃C₂T_x.

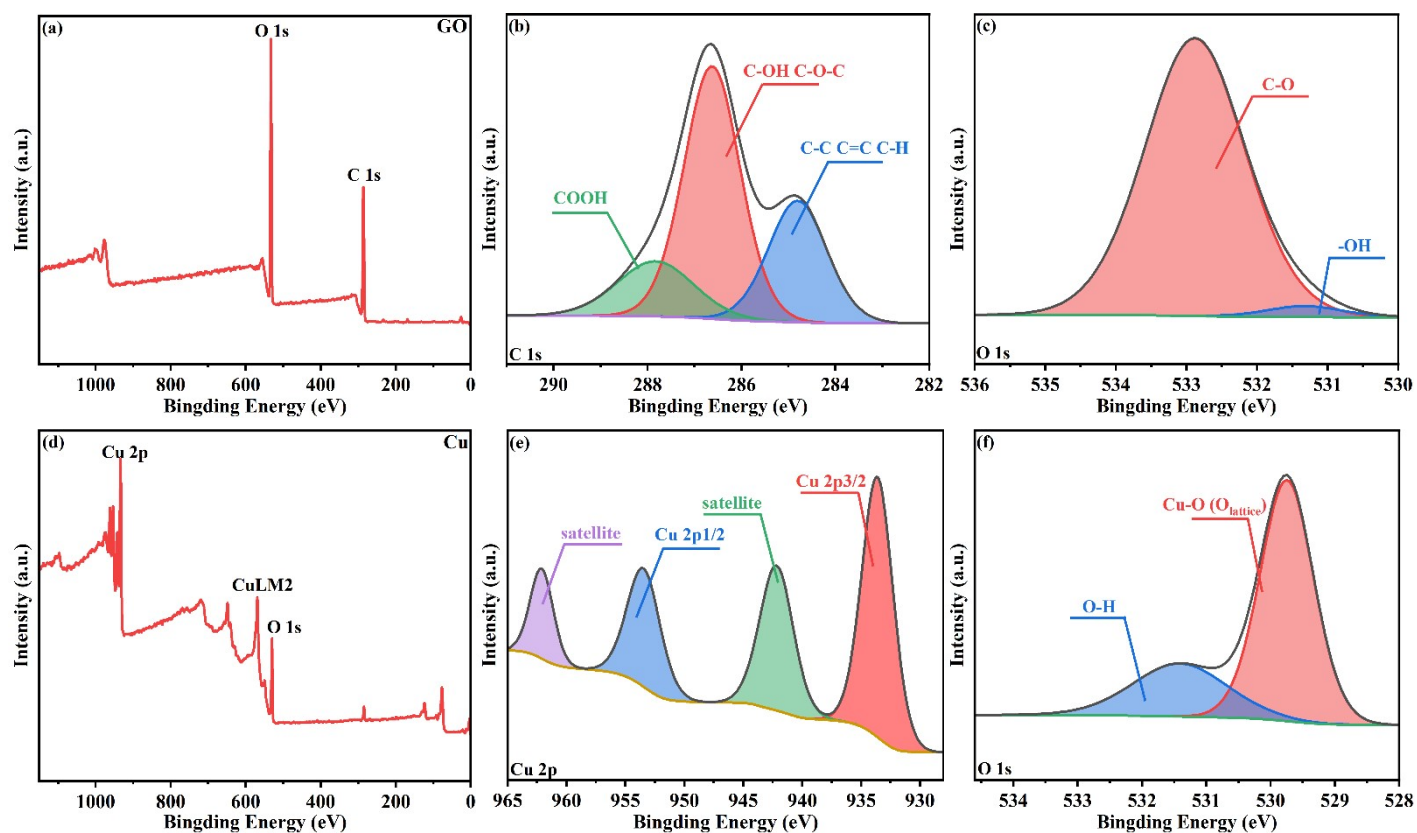


Fig. S5. XPS survey spectra of (a) GO. High-resolution XPS spectra of (b) C 1s, (c) O 1s of GO. XPS survey spectra of (d) CuO. High-resolution XPS spectra of (e) Cu 2p, (f) O 1s of CuO.

As shown in **Fig. S6a**, the characteristic peaks of D and G band near 1360 and 1590 cm^{-1} are reflected in the GO and I-GO/CuO complex, while in **Fig. S6b**, each corresponding peak in $\text{Ti}_3\text{C}_2\text{T}_x$ and I- $\text{Ti}_3\text{C}_2\text{T}_x/\text{CuO}$ is represented correspondingly, which indicates the generation of the complex. Meanwhile, the corresponding peak intensity of I-GO/CuO I- $\text{Ti}_3\text{C}_2\text{T}_x/\text{CuO}$ and spectrum are much weaker than that of GO and $\text{Ti}_3\text{C}_2\text{T}_x$. This may be related to the encapsulation structure of I-GO/CuO I- $\text{Ti}_3\text{C}_2\text{T}_x/\text{CuO}$.

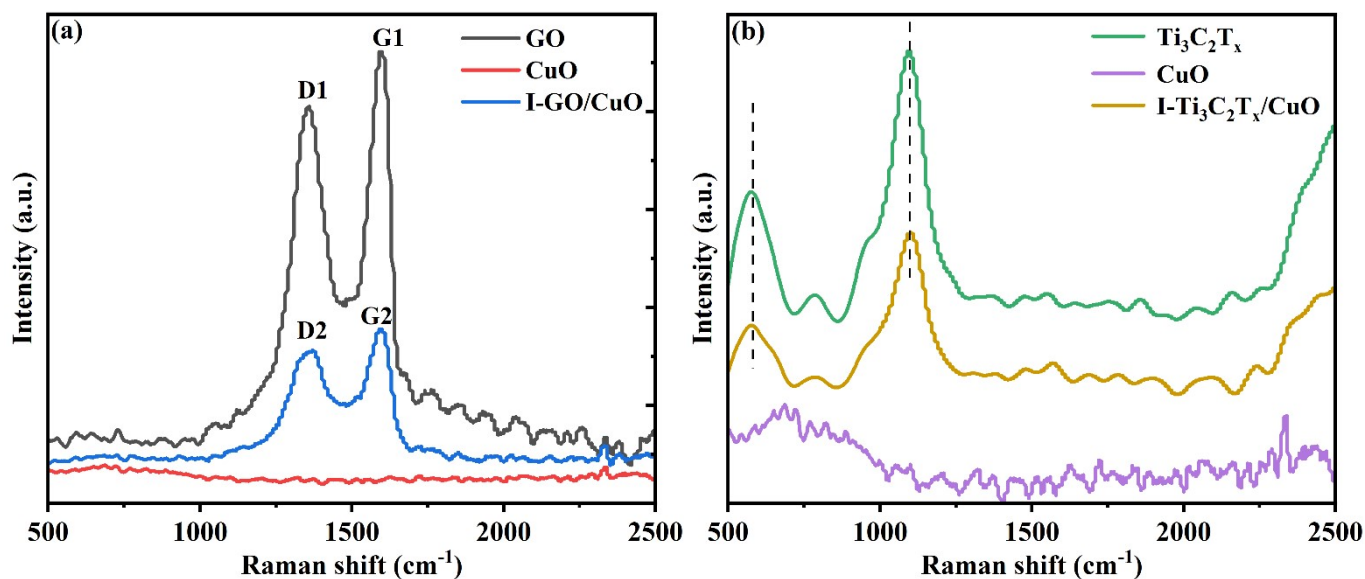


Fig. S6. Raman spectra of (a) GO, CuO, I-GO/CuO. (b) $\text{Ti}_3\text{C}_2\text{T}_x$, CuO, I- $\text{Ti}_3\text{C}_2\text{T}_x/\text{CuO}$.

Catalysis performance

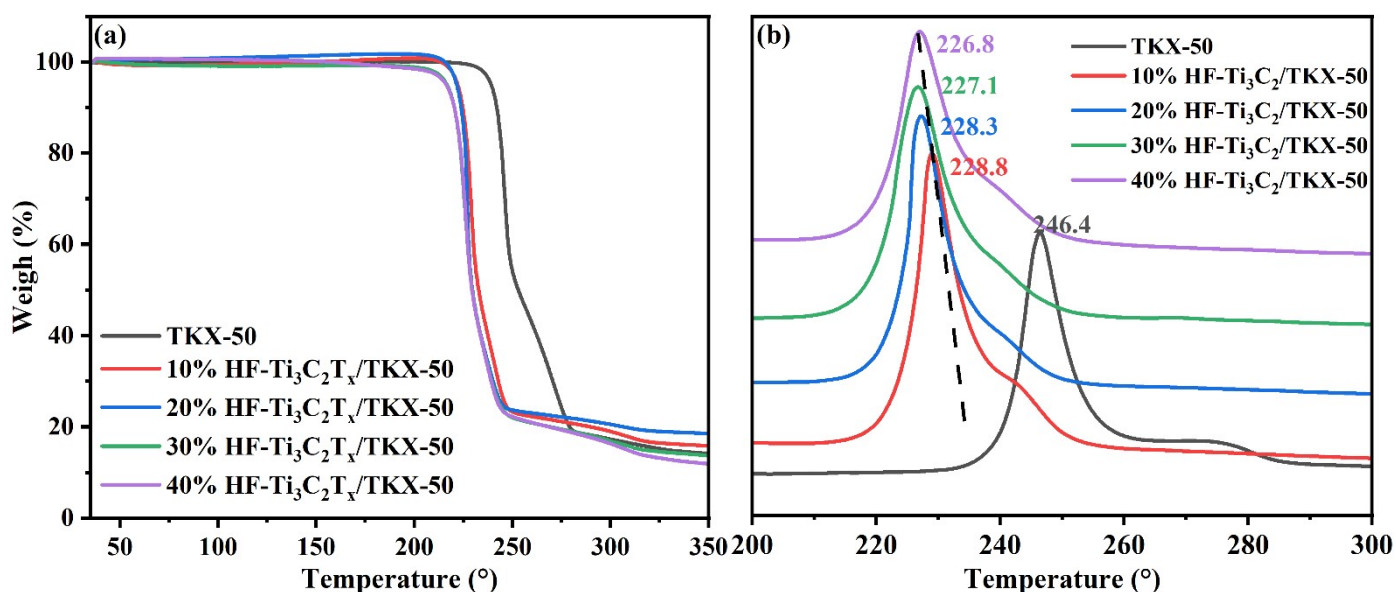
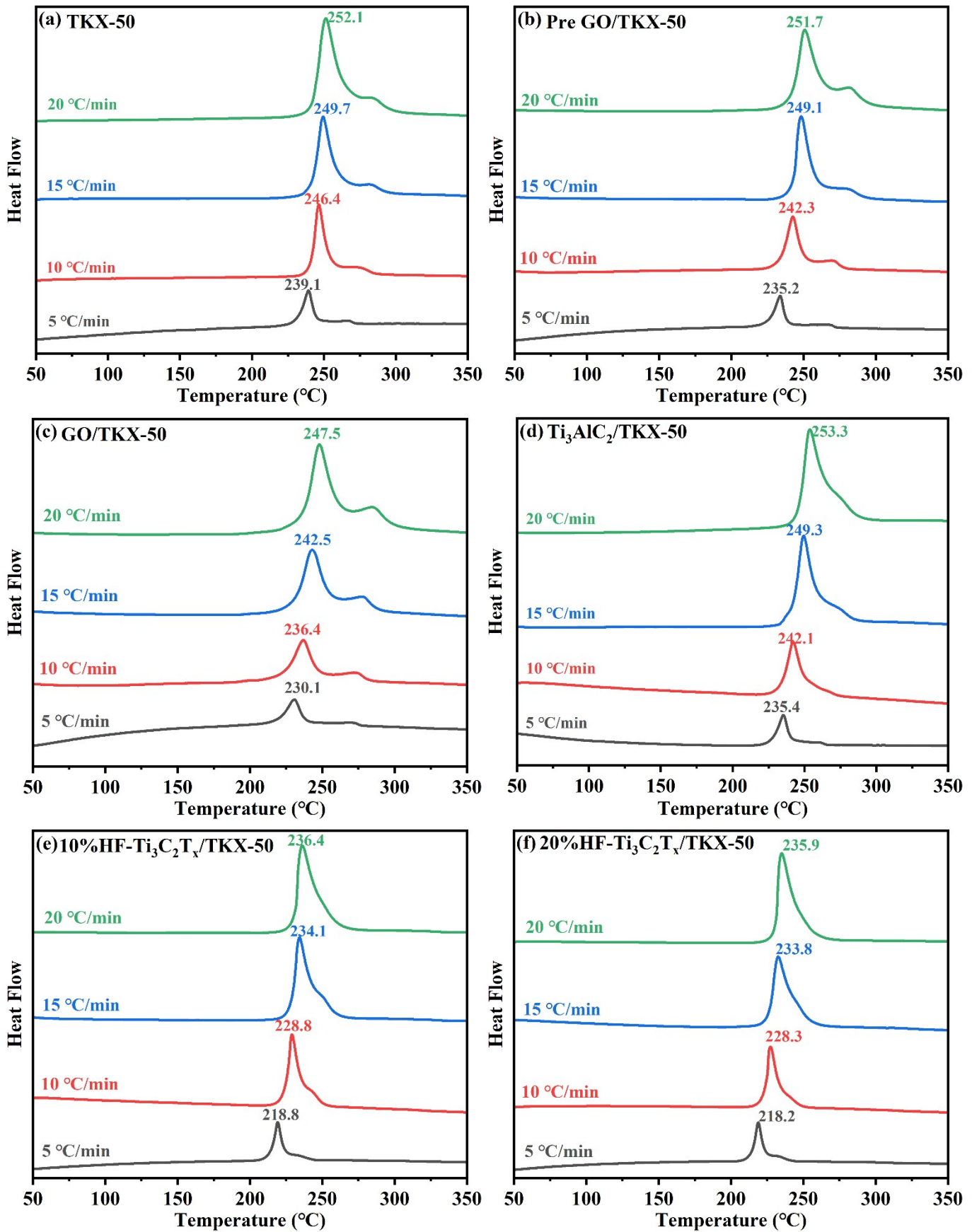
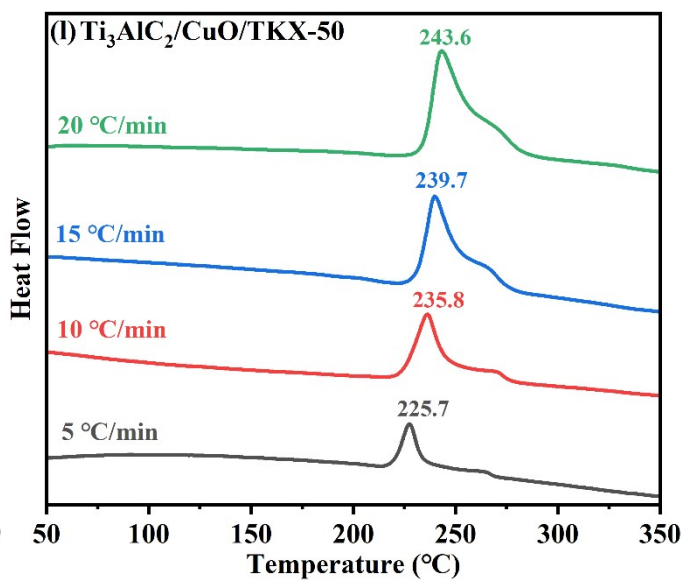
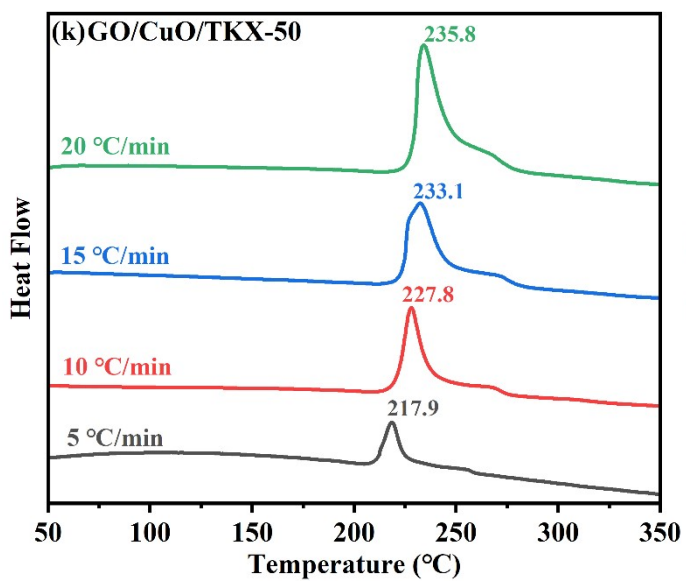
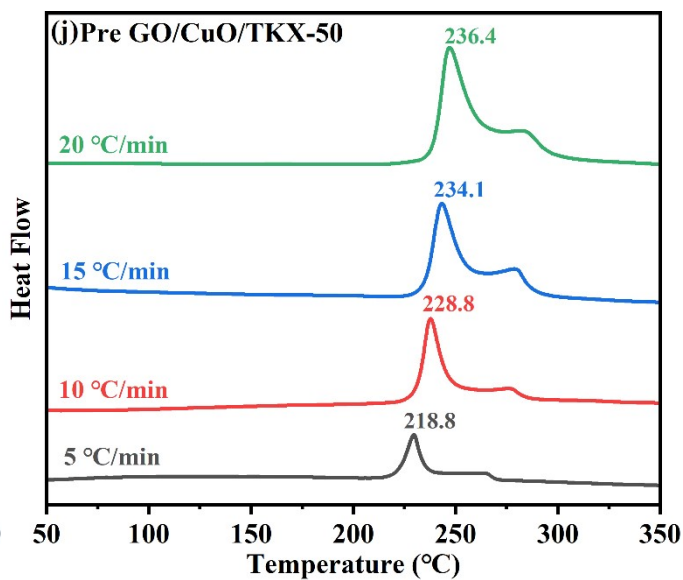
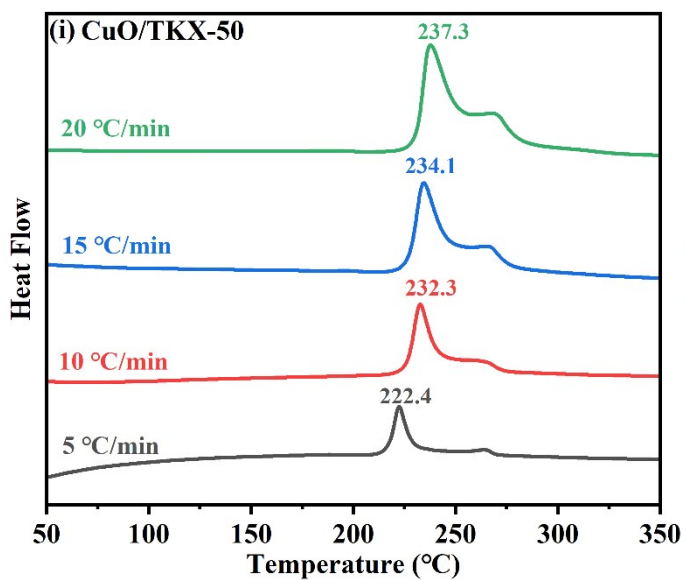
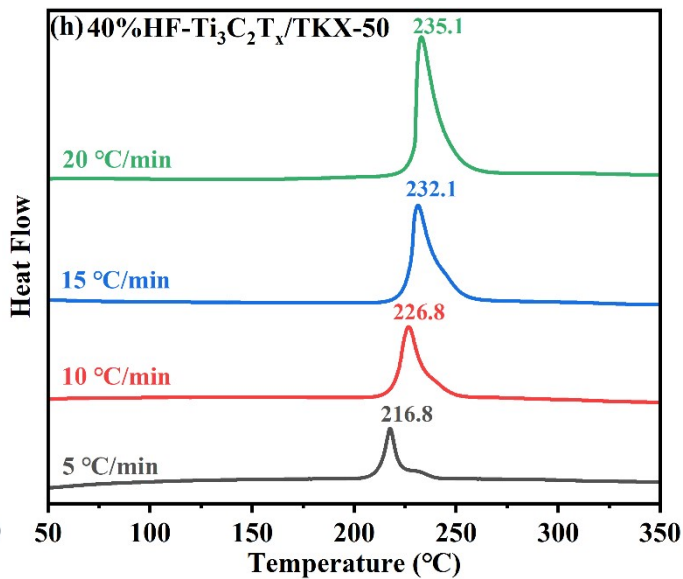
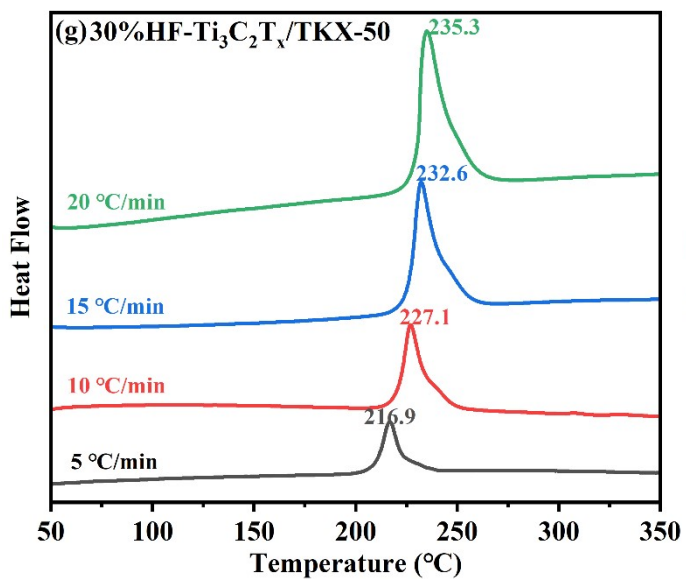


Fig. S7. $10^{\circ}\text{C}/\text{min}$ heating rate (a) TG curves of 10%HF- $\text{Ti}_3\text{C}_2\text{T}_x$, 20%HF- $\text{Ti}_3\text{C}_2\text{T}_x$, 30%HF- $\text{Ti}_3\text{C}_2\text{T}_x$, 40%HF- $\text{Ti}_3\text{C}_2\text{T}_x$. (b) DSC curves of 10%HF- $\text{Ti}_3\text{C}_2\text{T}_x$, 20%HF- $\text{Ti}_3\text{C}_2\text{T}_x$, 30%HF- $\text{Ti}_3\text{C}_2\text{T}_x$, 40%HF- $\text{Ti}_3\text{C}_2\text{T}_x$.

Catalysis mechanism





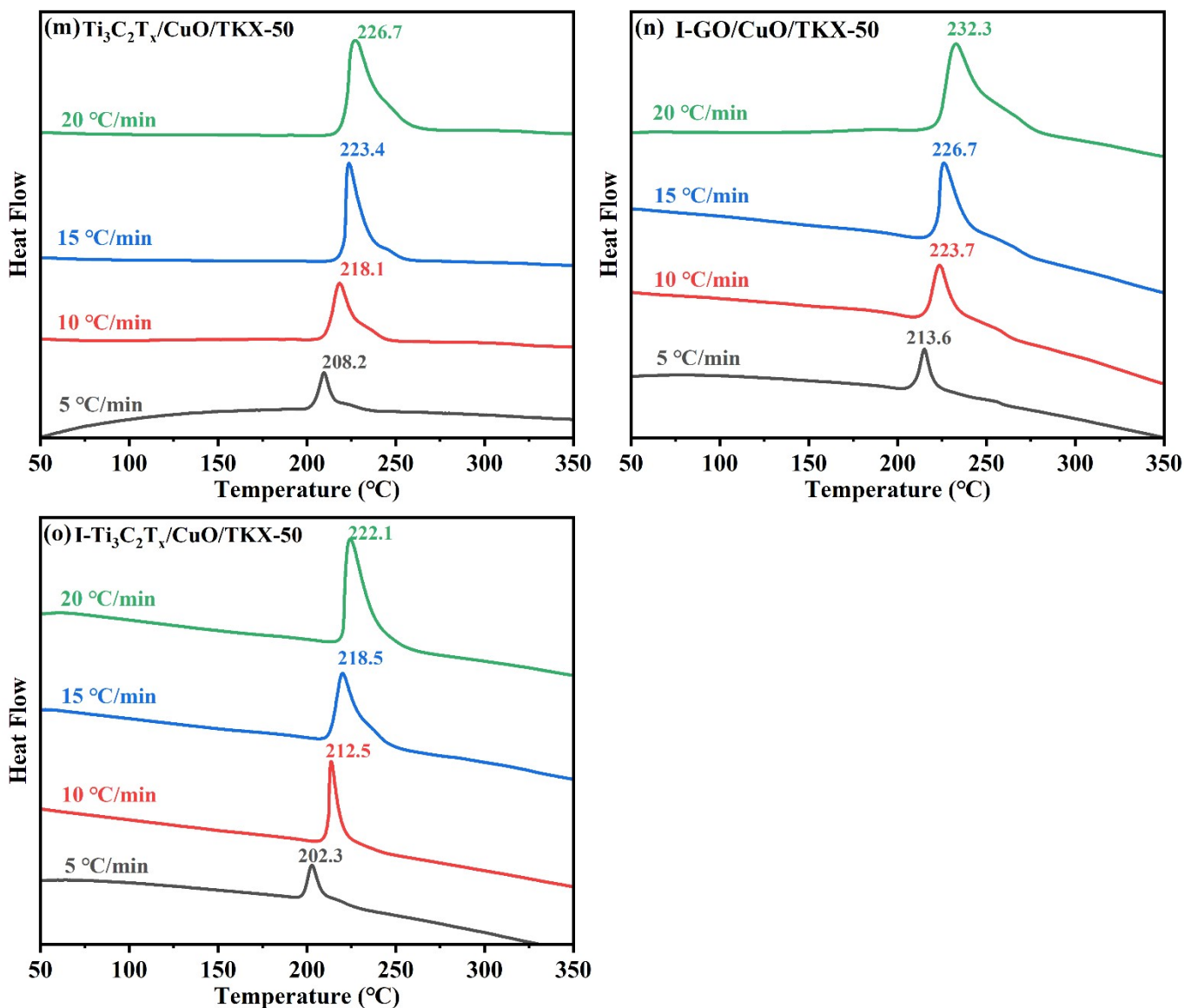


Fig. S8 DSC curves of (a) TKX-50, (b) Pre GO/TKX-50, (c) GO/TKX-50, (d) $\text{Ti}_3\text{AlC}_2/\text{TKX-50}$, (e) 10%HF- $\text{Ti}_3\text{C}_2\text{T}_x/\text{TKX-50}$, (f) 20%HF- $\text{Ti}_3\text{C}_2\text{T}_x/\text{TKX-50}$, (g) 30%HF- $\text{Ti}_3\text{C}_2\text{T}_x/\text{TKX-50}$, (h) 40%HF- $\text{Ti}_3\text{C}_2\text{T}_x/\text{TKX-50}$. (i) CuO/TKX-50 (j)Pre GO/CuO/TKX-50 (k) GO/CuO/TKX-50 (l) $\text{Ti}_3\text{AlC}_2/\text{CuO/TKX-50}$ (m) $\text{Ti}_3\text{C}_2\text{T}_x/\text{CuO/TKX-50}$ (n) I-GO/CuO/TKX-50 (o) I- $\text{Ti}_3\text{C}_2\text{T}_x/\text{CuO/TKX-50}$

Heating rate $\text{K/min} = ^\circ\text{C/min}$, $T_p(\text{K}) = 273.15 + T_p(^{\circ}\text{C})$

Table S1. Thermal decomposition temperature established using DSC and Kissinger E_a calculations of energetic compounds with the MXene catalysts

Sample	β (K/min)	T_p (K)	$1000/T_p$	$\ln(\beta/T_p^2)$	E_a (kJ/mol)	R^2
TKX-50	5	512.25	1.9521717	-10.8681876	228.3	0.9913
	10	519.55	1.9247425	-10.2033410		
	15	522.85	1.9125944	-9.81053903		
	20	525.25	1.9038553	-9.53201640		
Pre GO/TKX-50	5	508.35	1.9671486	-10.8529024	170.6	0.9828
	10	515.45	1.9400523	-10.1874955		
	15	522.25	1.9147917	-9.8082426		

	20	524.85	1.9053062	-9.5304927		
GO/TKX-50	5	503.25	1.9870839	-10.8327362	163.4	0.9751
	10	509.55	1.9625159	-10.1644708		
	15	515.65	1.9392999	-9.7828062		
	20	520.65	1.9206760	-9.5144237		
Ti ₃ AlC ₂ /TKX-50	5	508.55	1.9663749	-10.8536891	160.1	0.9722
	10	515.25	1.9408054	-10.1867193		
	15	522.45	1.9140587	-9.8090083		
	20	526.45	1.8995156	-9.53658044		
10%HF-Ti ₃ C ₂ T _x /TKX-50	5	491.95	2.0327269	-10.78731626	150.8	0.9833
	10	501.95	1.9922303	-10.13441593		
	15	507.25	1.9714144	-9.749957756		
	20	509.55	1.9625159	-9.471323693		
20%HF-Ti ₃ C ₂ T _x /TKX-50	5	491.35	2.0352091	-10.7848755	148.6	0.9803
	10	501.45	1.9942167	-10.13242271		
	15	506.95	1.9725811	-9.7487745		
	20	509.05	1.9644435	-9.4693602		
30%HF-Ti ₃ C ₂ T _x /TKX-50	5	490.05	2.0406081	-10.7795769	141.1	0.9887
	10	500.25	1.9990005	-10.1276308		
	15	505.75	1.9772614	-9.7440347		
	20	508.45	1.9667617	-9.4670014		
40%HF-Ti ₃ C ₂ T _x /TKX-50	5	489.95	2.0410245	-10.7791687	146.1	0.9924
	10	499.95	2.0002000	-10.1264310		
	15	505.25	1.9792182	-9.7420565		
	20	508.25	1.9675356	-9.4662146		
CuO/TKX-50	5	495.55	2.0179598	-10.8018986	169.6	0.9913
	10	505.45	1.9784350	-10.1483131		
	15	508.45	1.9667617	-9.7546835		
	20	511.85	1.9536973	-9.4803309		
Pre GO/CuO/TKX-50	5	491.95	2.0327269	-10.7873162	150.7	0.9833
	10	501.95	1.9922303	-10.1344159		
	15	507.25	1.9714144	-9.7499577		
	20	509.55	1.9625159	-9.4713236		
GO/CuO/TKX-50	5	491.05	2.0364525	-10.7836544	149.8	0.9896
	10	500.95	1.9962072	-10.1304275		
	15	505.25	1.9753086	-9.7460110		
	20	507.95	1.9648295	-9.4689672		
Ti ₃ AlC ₂ /CuO/TKX-50	5	498.85	2.0046106	-10.8151729	158.1	0.9878
	10	508.95	1.9648295	-10.1621144		
	15	512.85	1.9498878	-9.7719166		
	20	516.75	1.9351717	-9.4993861		
Ti ₃ C ₂ T _x /CuO/TKX-50	5	481.35	2.0774903	-10.7437514	141.7	0.9929
	10	491.25	2.0356234	-10.0913212		
	15	496.55	2.0138958	-9.7073181		
	20	499.55	2.0018016	-9.4316831		
I-GO/CuO/TKX-50	5	486.75	2.0544427	-10.7660633	146.9	0.9736
	10	496.85	2.0126798	-10.1139912		
	15	499.85	2.0006001	-9.7205659		

	20	505.45	1.9784350	-9.4551659		
I-Ti ₃ C ₂ T _x /CuO/TKX-50	5	475.45	2.103270586	-10.71908554	127.6	0.9978
	10	485.65	2.059096057	-10.06839131		
	15	491.65	2.033967253	-9.687483961		
	20	495.25	2.019182231	-9.414393098		

1. Cao, Y.; Deng, Q.; Liu, Z.; Shen, D.; Wang, T.; Huang, Q.; Du, S.; Jiang, N.; Lin, C.-T.; Yu, J., Enhanced thermal properties of poly(vinylidene fluoride) composites with ultrathin nanosheets of MXene. *RSC Advances* **2017**, 7 (33), 20494-20501.